



LAWRENCE
LIVERMORE
NATIONAL
LABORATORY

Chemistry & formation of the Bielby layer during polishing of fused silica glass

T. I. Suratwala, W. A. Steele, L. L. Wong, M. D. Feit, P. E. Miller, R. J. Dylla-Spears, N. Shen, R. P. DesJardin

January 21, 2015

Journal of the American Ceramic Society

Disclaimer

This document was prepared as an account of work sponsored by an agency of the United States government. Neither the United States government nor Lawrence Livermore National Security, LLC, nor any of their employees makes any warranty, expressed or implied, or assumes any legal liability or responsibility for the accuracy, completeness, or usefulness of any information, apparatus, product, or process disclosed, or represents that its use would not infringe privately owned rights. Reference herein to any specific commercial product, process, or service by trade name, trademark, manufacturer, or otherwise does not necessarily constitute or imply its endorsement, recommendation, or favoring by the United States government or Lawrence Livermore National Security, LLC. The views and opinions of authors expressed herein do not necessarily state or reflect those of the United States government or Lawrence Livermore National Security, LLC, and shall not be used for advertising or product endorsement purposes.

Chemistry & formation of the Bielby layer during polishing of fused silica glass

**T. Suratwala*, R. Steele, L. Wong, M. Feit, P.E. Miller,
R. Dylla-Spears, N. Shen, R. Desjardin**

Lawrence Livermore National Laboratory, P.O. Box 808, Livermore, CA 94551, USA

*Corresponding author: suratwala1@llnl.gov

The chemical characteristics and the proposed formation mechanisms of the modified surface layer (called the Bielby layer) on polished fused silica glasses are described. Fused silica glass samples were polished using different slurries, polyurethane pads, and at different rotation rates. The concentration profiles of several key contaminants, such as Ce, K and H, were measured in the near surface layer of the polished samples using Secondary Ion Mass Spectroscopy (SIMS). The penetration of K, originating from KOH used for pH control during polishing, *decreased* with increase in polishing material removal rate. In contrast, penetration of the Ce and H *increased* with increase in polishing removal rate. In addition, Ce penetration was largely independent of the other polishing parameters (e.g., particle size distribution and the properties of the polishing pad). The resulting K concentration depth profiles are described using a two-step diffusion process: (1) steady-state moving boundary diffusion (due to material removal during polishing) followed by (2) simple diffusion during ambient post-polishing storage. Using known alkali metal diffusion coefficients in fused silica glass, this diffusion model predicts concentration profiles that are consistent with the measured data at various polishing material removal rates. On the other hand, the observed Ce profiles are inconsistent with diffusion based transport. Rather we propose that Ce penetration is governed by the ratio of Ce-O-Si and Si-O-Si hydrolysis rates; where this ratio increases with interface temperature (which increases with polishing material removal rate) resulting in greater Ce penetration into the Bielby layer. Calculated Ce surface concentrations using this mechanism are in good agreement to the observed change in measured Ce surface concentrations with polishing material removal rate. These new insights into the chemistry of the Bielby layer, combined together with details of the single particle removal function during polishing, are used to develop a more detailed and quantitative picture of the polishing process and the formation of the Bielby layer.

1. Introduction

During the polishing of metals, crystals, and glasses, a modified amorphous surface layer is formed which ranges in thickness from a few nanometers to a micron. This layer is often referred to as the Bielby layer; although this name originally referred only to metal polished layers [1]. For polished glass surfaces, this layer has also been referred to as the polishing layer, the modified layer, and/or the hydrated layer.

The Bielby layer on glasses contains elevated levels of impurities whose concentration, as measured by secondary ion mass spectroscopy (SIMS), typically decays exponentially to the bulk concentration within a few tens of nanometers of the surface [2;3]. Sensitive optical reflectivity [4] and x-ray reflectivity [5] measurements indicate that the refractive index of this layer is typically 0.003-0.005 higher than the bulk material. The Bielby layer associated with silicate glasses can be removed by chemical etching (e.g., using HF acid) or modified by chemically leaching the cations (e.g., using mineral acids such as nitric acid) [6;7;8;4].

Trogolo et. al.[9] were able to successfully image the Bielby layer of silica glass in cross section using transmission electron microscopy. They showed the presence of two distinct surface layers, one that was 3-4 nm thick followed by a 15-20 nm deeper layer. More recently, Liao et. al.[10] performed similar measurements using FE-SEM. To date, no direct measurement of water penetration in the polishing layer has been reported, even though it is largely accepted that hydration is occurring. Wakabayashi and Tomozawa [11] presented indirect evidence that H₂O penetration is likely occurring.

The most accepted mechanisms associated with the polishing of glass surfaces, which in turn control the formation of the Bielby layer, involve the interplay of both chemical and mechanical interactions. These include the condensation & hydrolysis reactions between polishing slurry particles and glass surface [12], hydration of glass oxides [12;13], and nm scale plastic deformation [14]. Many questions remain regarding the characteristics and formation of the Bielby layer during glass polishing. Some of these include: (1) what is the mechanism (e.g., by impurity diffusion and reaction, by direct reaction layer formation, or by re-deposition) by which impurities are incorporated into the surface layer?; (2) how do polishing parameters influence the depth of the Bielby layer?; (3) what are the structural changes in the surface layer relative to the to the bulk silica glass?; (4) how are its mechanical & chemical properties different from the bulk?; and (5) how does this layer influence the single slurry particle removal function and the resulting polished surface roughness of the polished glass? In the following study, we attempt to answer the first three questions by measuring changes in the elemental composition of the near surface layer as a function polishing parameters. Using this information, a more detailed chemical and structural model of how material removal occurs during polishing is formulated.

2. Experimental

Sample Preparation. Fused silica workpieces (50 mm diameter x 10 mm thick; Corning 7980, Corning, NY) were polished using the Convergent Polishing method [15] (baseline conditions: 0.6 psi applied pressure, 0.6 mL/min slurry feed rate (single pass), Stabilized Hastilite PO polishing slurry (Baume 5; pH adjusted to 9.5 using KOH) [16], 20 rpm optic and lap rotation rate, 300 mm lap diameter, 50 mm linear stroke distance). The lap rotation rate (5-40 rpm), polishing pad (MHN 50 mil; Chem-Pol; Optivision; Polytex (Eminess Technologies, Scottsdale, AZ), polishing slurry (Stabilized Hastilite PO Ceria (Universal Photonics Inc, Hicksville, NY), NanoArc 6752 (Nanophase Technologies Corp, Romeoville, IL), Ultra-Sol S27 (Eminess Technologies, Scottsdale, AZ)), and slurry pH (6-12) were adjusted for the various samples. The material removal rates were determined gravimetrically. An additional set of fused silica samples were etched 26 μm with $\text{NH}_4\text{F}:\text{HF}$ (buffered oxide etch 6:1 3x diluted in water for 14 hrs) [7] and then soaked in either Stabilized Hastilite PO polishing slurry or 10M KOH. Table 1 summarizes the samples prepared for this study.

SIMS Characterization. Depth resolved Secondary Ion Mass Spectroscopy (SIMS) measurements of Ce and K were performed by the Evans Analytical Group (EAG) using an IONTOF TOF SIMS 5 which incorporated the use of a Bi^+ source operated at 30 kV and a O_2 sputtering ion beam. A $50 \times 50 \mu\text{m}^2$ analysis zone centered within a $200 \times 200 \mu\text{m}^2$ sputtered zone (15.6 Angstroms/sec) was used for all Ce and K depth profile measurements. H SIMS was also performed by EAG using a Phi Adept 1010 dynamic SIMS using Cs bombardment and negative ion detection. Concentration measurements were calibrated using an ion implanted fused silica reference sample.

SEM Characterization. Field Emission Scanning Electron Microscopy (FE-SEM) was performed on the polished surface of several fused silica samples using a FEI XL-30 SFEG operated at 20 KeV. These samples were coated with Au, prior to analysis to reduce charging.

3. Results

The depth profiles of K and Ce for a series of fused silica samples polished at different velocities (and hence different polishing removal rates) are shown as a pair of semi-log plots in Figures 1a & b. Note the bulk glass Si concentration was measured at uniform value of 2×10^{22} atoms/ cm^3 (not shown in plot), while the noise floor of each analyte is $\sim 10^{16}$ atoms/ cm^3 . K penetration into the glass surface was significantly greater ($\sim 500\text{-}900$ nm) than the Ce penetration ($\sim 20\text{-}100$ nm). Also, the surface concentration for both impurities varied significantly from 6×10^{16} to 2×10^{20} atoms/ cm^3 with changes in polishing conditions.

Finally, and most significantly, the K penetration was observed to *decrease* with increase in polishing material removal rate, while the Ce penetration was found to *increase* as a function of material removal rate.

Figure 2a shows a series of Ce depth profiles for several additional of fused silica samples which were polished using different slurries and different polishing pads. As observed in Fig. 1a, the depth of Ce penetration is found to vary significantly depending upon the polishing process used. As shown with sample NP1 in Fig. 2a, simply soaking a fused silica sample in Ceria slurry does not allow Ce to penetrate into the surface of the polished sample. This suggests that some combination of mechanical loading and lateral motion of the particle during polishing is required to transport the Ce into the near surface layer of the glass. Again, the dominant polishing variable affecting the Ce penetration is the polishing material removal rate. This is illustrated in Fig. 2b, which plots the Ce surface concentration as a function of polishing material removal rate for all the samples summarized in Table 1.

Some additional K depth profiles are shown in Figures 3a and 3b. Fig. 3a shows that soaking etched fused silica samples in KOH results in significant penetration of KOH even without polishing. This is unlike the behavior observed when glass is soaked in an aqueous solution of Ce polishing slurry as shown in Fig. 2a. Fig. 3b illustrates that after polishing, K continues to penetrate into the glass during storage under ambient conditions.

The H depth profiles for two polished fused silica samples are shown in Figure 4. Here the instrumental noise floor is much higher $\sim 10^{19}$ atoms/cm³. Hence, the actual penetration depth of H into surface cannot be determined. However, the results confirm high surface concentration of H of $\sim 1\text{-}3 \times 10^{20}$ atom/cm³ (i.e., 10,000 to 30,000 ppm) which is likely due to H₂O penetration. To the authors' best knowledge, this is the first experimental confirmation of H₂O penetration into glass surface during polishing, confirming previous hypothesized hydration processes during polishing [12;13]. Also, note that H penetration cannot be accounted for simply by KOH penetration alone, since the surface H concentration was much higher than the K surface concentration. That is, the present data suggest it is likely that the majority of H observed is due to the transport of H₂O originating from the aqueous polishing slurry.

Finally in Figure 5, a high magnification FE-SEM image is shown of the glass surface. In contrast to the findings by Liao et. al. [10] who showed significant spatial variations in the penetration of impurities at a scale length of several microns using a similar measurement, the polished samples observed this study are much more uniform at this scale length.

4. Discussion

4.1 Diffusion vs Chemical Reactivity

One potential mechanism of incorporating cation impurities into the glass surface during polishing is diffusion. If the Bielby layer formation is diffusion induced, then there should be a steady-state relationship between material removal rate and the diffusion mass transfer of the impurity species. At steady-state, the diffusion flux of the impurities into the glass is equal to the flux of impurities removed due to removal of the surface during polishing. This balance is given by:

$$J_{diffusion} = J_{materialremoval} \quad (1a)$$

$$C \frac{dh}{dt} = D \frac{dC}{dx} \quad (1b)$$

where C is the impurity concentration, dh/dt is the material removal rate, D is the impurity cation diffusivity, and x is the depth into the moving glass surface. Note the right hand side of Eq. (1b) is simply Fick's first law. Using the Preston's material removal equation [6] and solving Eq. (1b) gives:

$$\frac{dh}{dt} = k_p \sigma_a V_r \cong \frac{D}{t_{Bielby}} \quad (2)$$

where k_p is the Preston constant, σ_a is the applied pressure, V_r is the relative velocity during polishing, and t_{Bielby} is the effective thickness of the Bielby layer. This relationship suggests that increasing the material removal rate should result in a decrease in the Bielby layer thickness (i.e., decrease the relative penetration of a given impurity). From the results shown in Fig. 1a, K penetration is consistent with the behavior expected for diffusion, where K penetration decreases with increase in material removal rate. In contrast, the penetration of Ce into the near surface layer is inconsistent with a diffusion mechanism, because Ce penetration increases with increase in material removal rate (Fig. 1b). This suggests that another mechanism, such as by chemical reactivity, rather than diffusion, dominates the penetration of Ce into the glass surface. In the next two sections, a more detailed set of mechanisms for K penetration by diffusion and Ce penetration due to chemical reactivity are proposed and discussed.

4.2 K penetration by two-step diffusion

As discussed above, K diffusion into the surface of the fused silica glass occurs both during the polishing process as well as during subsequent post-polishing, room temperature storage. Hence K penetration into the surface is modeled as a two-step diffusion process. During the first (polishing) step, diffusion occurs at a moving surface boundary and steady-state is reached [17]. Consider a fused silica surface in the presence of K ions from the slurry with a constant surface moving boundary of dh/dt (i.e., the polishing thickness removal rate). Using a concentration independent diffusion coefficient (D) for K in a semi-infinite solid in one

dimension (x), the steady-state diffusion process with moving boundary is proposed to simply follow an advection diffusion model:

$$\frac{d}{dx} \left(D \frac{dC_K}{dx} + \frac{dh}{dt} C_K \right) = 0 \quad (3)$$

where C_K is the K concentration. The solution to Eq. (3) has the form:

$$C_K(x) = \frac{A}{\left(\frac{dh}{dt}\right)} \exp \left(\frac{-\left(\frac{dh}{dt}\right)x}{D} \right) \quad (4)$$

where A is constant. The pre-exponential term is the surface concentration which is removal rate dependent in conformity to the experimental observation. Additionally, the form of Eq. (3) implies the magnitude of the diffusive flux $D \cdot dC_K/dx$ is independent of removal rate. Also, note in Eq. (4) that the value of the exponential term will change with dh/dt . In other words, the slope of K depth profiles on a semi-log plot should change with removal rate. Clearly the measured data does not show a significant change in slope (see Figure 1a) even though the removal rate changed by $\sim 10x$. Again, this suggests that a single step diffusion process is not sufficient to describe the observed data.

In the second step of diffusion, during storage, the source of K is now removed and the silica glass surface boundary is fixed. In this case, the time-dependent K diffusion is determined by Fick's second law in the form:

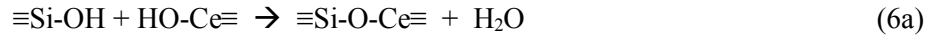
$$\frac{d}{dx} \left(D \frac{dC_K}{dx} \right) = \frac{dC_K}{dt} \quad (5)$$

with the boundary conditions of zero concentration in the bulk glass and no removal of K from the surface of the glass. The authors were unable to find literature values for the room temperature K diffusion in fused silica. However, Na ($r=0.95$ Angstroms) diffusion (expected to be similar to K ($r=1.33$ Angstroms) near room temperature was measured by Frischat et. al. [16]. Extrapolating their data to room temperature gives an approximate diffusivity of $\sim 10^{-16}$ cm²/sec. Using this diffusivity value for both diffusion steps and a best fit value of $A=10^{21}$ cm⁻³/($\mu\text{m/hr}$), the calculated diffusion curves are compared with the measured data two weeks after polishing at different removal rates (see Fig. 6). The dashed lines are the calculated concentration depth profiles immediately after polishing while the solid lines are the calculated concentration profiles after two weeks of storage. The general shape, penetration depth, and material removal rate dependence of the two-step diffusion model is in good agreement with the experimental data, using only one fitting parameter. There is, however, a deviation in the detailed shape of final measured diffusion profiles with the two-step model using a constant diffusion coefficient (see Fig. 6). The authors hypothesize this deviation is due to changes in

the diffusivity (D) of K with depth (x) due to changes in the structure of the glass in the Bielby layer with depth possibly resulting from OH penetration.

4.3 Ce penetration by chemical reactivity

In contrast to the behavior of the K penetration, Ce penetration into the fused silica surface *increases* with polishing material removal rate. In fact, a quantitative correlation exists between the measured Ce depth profile and the measured material removal rate (Fig. 2b). It is known that ceria plays a key role in the removal of silica from the glass surface during the polishing process. The most widely accepted chemical mechanism is by condensation and subsequent hydrolysis reactions given by [12]:



where reaction (6a) is the condensation reaction between the Si-OH silica surface and Ce-OH ceria particle surface, and reaction (6b) is the subsequent hydrolysis of the Si-O-Si bond leading to the removal of silica from the glass surface. Here we propose another possible reaction where the hydrolysis can occur at the Ce-O-Ce bond leaving Ce behind on the silica surface, given by:



Clearly for material removal to occur during polishing, the rate of reaction (6b) must be much greater than reaction (6c).

Consider the rate of deposition of Ce (R_{dep}) due to reaction (6c) and the rate of removal of Ce (R_{rem}) due to reaction (6b) from the moving silica surface during polishing. At steady-state, these rates will be equal:

$$R_{\text{dep}} = R_{\text{rem}} \quad (7a)$$

which can be rewritten in the form:

$$2a v_p \rho_p S_p r_{\text{Ce:Si}} = 2a v_p d \rho_p [\text{Ce}]_s \quad (7b)$$

where 2a is the contact diameter of a spherical polishing particle, v_p is the velocity of the polishing particle, ρ_p is the particle number density per unit area, S_p is the areal number density of Si atoms, d is removal depth or the bond length, $r_{\text{Ce:Si}}$ is the hydrolysis reaction rate ratio between Ce-O-Ce and Si-O-Si, and $[\text{Ce}]_s$ is resulting the steady state Ce concentration at the surface. Note that $2av_p$ is the *areal* contact per slurry particle per unit time and $2av_p d$ is the *volumetric* removal per slurry particle per unit time. Simplifying Eq. (7b) gives:

$$[\text{Ce}]_s = \frac{S_p r_{\text{Ce:Si}}}{d} \quad (8)$$

which suggests that the steady state Ce surface concentration will be dominated by the ratio of the two hydrolysis reactions ($r_{\text{Ce:Si}}$), since S_p (areal density of Si atoms) and d (removal depth) would be to be largely constant.

To account for changes in the Ce surface concentration with changes in material removal rate, we propose that the hydrolysis reaction ratio ($r_{\text{Ce:Si}}$) changes with interface temperature which is a function of the material removal rate. The interface temperature has been previously described for a single sliding particle, generating frictional heat at the moving contact interface given by [17;18;19]:

$$T = \frac{1.464 a Q}{k_{\text{SiO}_2} \sqrt{\pi(0.874 + Pe)}} \quad (9a)$$

where:

$$Q = \frac{\mu P v_p}{\pi a^2} \quad (9b)$$

$$Pe = \frac{v_p a \rho_{\text{SiO}_2} C_{\text{SiO}_2}}{2 k_{\text{SiO}_2}} \quad (9c)$$

where a is the contact radius, Q is the frictional heat flux, P is the applied load, v_p is the particle velocity, ρ_{SiO_2} is the silica mass density (2.2 gm/cm³), k_{SiO_2} is the thermal conductivity of silica (1.4 W/mK), C_{SiO_2} is the head capacity of silica (740 J/kgK), and Pe is the Peclet Number.

In a previous study, the average contact parameters were determined from polishing experiments and using a contact mechanics model, called the Ensemble Hertzian Gap Model [14], as $a=55$ nm and $P=10^{-4}$ N (plastic removal). In addition, the material removal rate is related to the workpiece velocity by the Preston Equation (see Eq. (2) [6] where the Preston Constant (k_p) is 2.2×10^{-13} m²/N and the applied pressure (σ_o) is 0.6 psi. Using Eqs. (9a-c) to get the velocity dependence of the temperature rise and assuming the workpiece velocity (V_r) is equal to the particle velocity (v_p), the calculated temperature rise as a function of material removal rate (from Eq. (2)) is shown in Figure 7. The results show that the particle-workpiece interface temperature increases at a rate 55 K for each 1 um/hr increase in removal rate. In a previous study [20], the global temperature rise was measured during polishing under very similar conditions leading to a temperature rise of 1-2 K. Because the total particle-workpiece contact area is small relative to the whole workpiece surface area, it is expected that the local interface temperature would be much higher than the global temperature of the system.

Next, we propose that $r_{\text{Ce:Si}}$ has an Arrhenius temperature dependence, then Eq. (8) can be rewritten as:

$$C_o = \frac{S_p}{d} r_o \exp\left(\frac{-E}{R T(dh/dt)}\right) \quad (10)$$

where r_o is the pre-exponential constant, E is the activation energy, $T(dh/dt)$ is the interface temperature as a function of removal rate (shown in Fig. 7). Figure 2b shows the comparison of the calculated Ce surface concentration (using $r_o=80$ and $E=10$ kcal/mole) with measured values from all SIMS results for each of the polishing samples. This model does a reasonable job matching the observed Ce surface concentration versus removal rate. The best fit activation energy value of $E=10$ kcal/mole appears to be a reasonable value since hydrolysis activation of Si-O-Si has been previously reported to have similar values [21].

4.4 Chemical-structural-mechanical model of the Bielby layer and the polishing process

The results of the present study together with previous work on polishing parameters [14], can be used to formulate a more detailed chemical-structural-mechanical picture of the Bielby layer and polishing process that leads to its formation (see Table 2 and Fig. 8). Consider the specific case where a fused silica sample is polished on a MHN polyurethane pad using ceria slurry, such as stabilized Hastilite PO ceria (see for example sample P1 in Table 1). As the workpiece is polished, the Bielby layer is formed as impurities such as water (observed mass spectrometrically as H) and elemental impurities, such as Ce and K, penetrate into the glass surface, ultimately leading to a concentration profile which exponentially decays into the depth of the sample. The concentrations of each of the impurities, as noted by just the surface concentrations in Table 2, are quite different. H is the highest having a H:Si ratio of 1:100, followed by Ce with Ce:Si ratio of 1:400, and then K with a K:Si ratio of 1:20,000. Given this, the depth of the Bielby layer is difficult to unambiguously define since each of these species penetrates to significantly different depths. Moreover, the depth a given species penetrates may be time and/or polishing rate dependent. For convenience, we define the depth of the Bielby layer in terms of the depth of Ce penetration. More specifically, for the present work we take the depth of the Bielby at the point where Ce concentration is no longer detectable from SIMS measurement noise floor of $\sim 10^{16}$ atoms/cm³. In this case, the depth is ~ 50 nm. Note, however, given the exponential decay in the concentration, the vast majority of the Ce is present within just the first few nanometers of the surface.

The bonding structure of the fused silica surface is more difficult to determine. The bulk structural information for silica glass has been previously well characterized by solid-state NMR by many researchers (e.g., [Y]). The Si Q species describes the quaternary oxygen tetrahedron in the glass structure, where Q⁴ represent 4 Si-O neighbors, Q³ represents 3 Si-O neighbors, etc. The greater the fraction of Q⁴, the more cross-linked structure of the glass. It is reasonable that K and H behave as network modifiers, decreasing the crosslinking of the glass structure. Similarly, Ce would be expected to behave as a network former [22]. By

assuming that all the K and H species detected in the surface layer act as network modifiers, one can compare the estimated distribution of Q species in the surface layer to that of bulk fused silica (see Table 2). As shown in Table 2, the resulting change in the calculated Q species ratio suggests only a minor reduction in crosslinking. This small change reflects the low abundance of ionic and atomic impurities such as H, Ce, and K relative to the number of Si and O atoms even in the near surface layer of the glass.

The mechanical aspects of the contact between a polishing particle and the glass surface can be determined using the results of our previous study [14]. Here the mechanics of particles loaded on glass surface were evaluated using the measured slurry particle size distribution and the Ensemble Hertzian Gap (EHG) model. The model is based on multiple Hertzian contacts of slurry particles at the workpiece-pad interface in which the effective interface gap is determined through an elastic load balance. Using this formulation, the load, penetration, and contact zone distributions were determined from the slurry particle size distribution. In addition, the removal function for a single sliding particle was experimentally determined in the course of this study [14]. The resulting parameters are summarized in Table 2; the average particle size (resulting in plastic type removal) was ~ 800 nm with an average load of 10^{-4} N resulting in an elastic contact zone of 110 nm, a penetration depth of 3.8 nm, and removal depth of 1 nm.

Combining these parameters with information from the present study and accounting for the material removal rate, allows the development of a schematic representation of the important chemical, structural, and mechanical aspects of the Bielby layer and the polishing process to be represented (Figure 8). Here a single ≈ 800 nm particle slides under load on the glass surface from left to right. The particle size, contact zone, penetration depth, and Bielby layer thickness are shown to scale. The presence of chemical impurities, such as H and Ce, in the surface layer is indicated by the colored dots; the density of which corresponds to the relative areal concentrations expected in the scale length of the model. The pictorial inserts represent a more detailed view of the glass structure both at and just below the particle-glass interface. Because of the exponential decay in the concentration of impurities, the Bielby layer resembles the bulk glass within just a few nanometers of the surface. Also, because the K concentration is so low it does not, on average, appear within the scale length of the model shown in Fig. 8.

5. Conclusions

SIMS based measurements of the depth profile of K, Ce and H impurities on the surfaces of fused silica glasses prepared under different polishing conditions reveal important chemical and physical characteristics of the near surface Bielby layer. For ions, such as K, penetration appears to occur as a two-step diffusion process. In contrast, ions such as Ce, which are active participants in the polishing process, the depth penetration appears to be consistent with a mechanism which depends on the relative rate of hydrolysis

between Ce-O-Si and Si-O-Si, where the ratio increases with interface temperature (which increases with polishing removal rate). Finally, using this insight, combined with mechanical loading information of individual polishing particles from a previous study, a more detailed chemical-structural-mechanical picture of the Bielby layer formation and polishing process has been formulated.

References

- [1] G. Beilby, *Aggregation and Flow of Solids*, Macmillan: London, 1921.
- [2] P. Miller, J. Bude, T. Suratwala, N. Shen, T. Laurence, W. Steele, J. Menapace, M. Feit, L. Wong, “Fracture-induced subbandgap absorption as a precursor to optical damage on fused silica surfaces” *Optics Letters* **35(16)** (2010) 2702-2704.
- [3] M. Kozlowski, J. Carr, I. Hutcheon, R. Torres, L. Sheehan, D. Camp, M. Yan, “Depth profiling of polishing-induced contamination on fused silica surface” *SPIE* **3244** (1997) 365-375.
- [4] M. Nostrand, J. Wolfe, D. Willard, “Detailed assessment of DOFAST Diffraction Efficiency Measurement Errors and Ramifications for Energy and Power Reporting” LLNL memo NIF-0176020-AA (2015).
- [5] W. Wallace, W. Wu, R. Carpio, “Chemical-mechanical polishing of SiO₂ thin films studied by X-ray reflectivity”, *Thin Solid Films* **280** (1996) 37-42.
- [6] F. Preston, “The structure of abraded glass surfaces”, *Trans Opt. Soc.* **23(3)** 141 (1922) 141.
- [7] T. Suratwala, P. Miller, J. Bude, W. Steele, N. Shen, M. Monticelli, M. Feit, T. Laurence, M. Norton, C. Carr, L. Wong, “HF-based etching Processes for improving laser damage resistance of fused silica optical surfaces”, *J. Am. Ceram. Soc.* **94(2)** (2011) 416-428.
- [8] P. Miller, T. Suratwala, J. Bude, N. Shen, W. Steele, T. Laurence, M. Feit, L. Wong, “Methods for globally treating silica optics to reduce optical damage”, US Patent 8313662 (November 20, 2012).
- [9] J. Trogolo, K. Rajan “Near surface modification of silica structure induced by chemical/mechanical polishing” *Journal of Materials Science* **29** (1994) 4554-58.
- [10] D. Liao, X. Chen, C. Tang, R. Xie, Z. Zhang, “Characteristics of hydrolyzed layer and contamination on fused silica during polishing” *Ceramics International* **40** (2014) 4470-4483.
- [11] H. Wakabayashi, M. Tomozawa, “Diffusion of water into silica glass at low temperature”, *J. Am. Ceram. Soc.* **72(10)** (1989) 1850-55.
- [12] L. Cook, “Chemical Processes in Glass Polishing,” *J. Non-Cryst. Solids* **120** (1990) 152–171.
- [13] M. Tomozawa, “Oxide CMP Mechanisms” *Solid State Technology* (July 1997) 169-175.

- [14] T. Suratwala, M. Feit, R. Steele, L. Wong, N. Shen, R. Dylla-Spears, R. Desjardin, D. Mason, P. Geraghty, P. Miller, S. Baxamusa "Microscopic removal function & the relationship between slurry particle size distribution & workpiece roughness during pad polishing" *J. Am. Ceram. Soc.* **97(1)** (2014) 81-91.
- [15] T. Suratwala, R. Steele, M. Feit, R. Desjardin, D. Mason, "Convergent Pad Polishing of Amorphous Silica", *International Journal of Applied Glass Science* **3(1)** (2012)14-28.
- [16] R. Dylla-Spears, L. Wong, P. Miller, M. Feit, W. Steele, T. Suratwala, "Charged micelle halo mechanism for agglomeration reduction in metal oxide polishing slurries" *Colloids and Surfaces A: Physicochem. Eng. Aspects* **447** (2014) 32–43.
- [17] J. Crank, *The Mathematics of Diffusion*, 2nd Ed (1975).
- [18] G. Frischat, "Sodium diffusion in SiO₂ Glass" *J. Am. Ceram. Soc.* **51(9)** (1968) 528-530.
- [19] Y. Chen, L. Zhang, "Polishing of polycrystalline diamond by the technique of dynamic friction, part 1: Prediction of the interface temperature rise", *J. of Machine Tool & Manufacture* **46(6)** (2006) 580-587.
- [20] J. Jaeger, "Moving source of heat and temperature at sliding contacts" *Proc. Royal Soc.* **76** (1942) 203-224.
- [21] X. Tian, F. Kennedy, "Maximum and average flash temperatures in sliding contacts" *AMSE Journal of Tribology* **116(1)** (1994) 167.
- [22] M. Cypriak, Y. Apeloig, "Mechanism of the acid-catalyzed Si-O bond cleavage in siloxanes and siloxanols. A theoretical Study" *Organometallics* **21(11)** (2002) 2165-2175.
- [23] T. Suratwala, M. Feit, R. Steele, L. Wong, L., "Influence of Temperature and Material Deposit on Material Removal Uniformity during Optical Pad Polishing" *J. Am. Ceram. Soc.* **97(6)** (2014) 1720–1727.
- [24] W. Kingery, H. Bowen, D. Uhlmann, "Introduction to Ceramics" John Wiley & Sons New York (1976).
- [25] H. Eckert, "Structural characterization of noncrystalline solids and glasses using solid state NMR" *Progress in Nuclear Magnetic Resonance* **24(3)** (1992) 159-293.

Acknowledgements

This work performed under the auspices of the U.S. Department of Energy by Lawrence Livermore National Laboratory under Contract DE-AC52-07NA27344 within the LDRD program. Special thanks to Ed Sedillo for performing the FE-SEM measurements. [LLNL-JRNL-666384]

Table 1: Polishing parameters and resulting material removal rate for each of the samples.

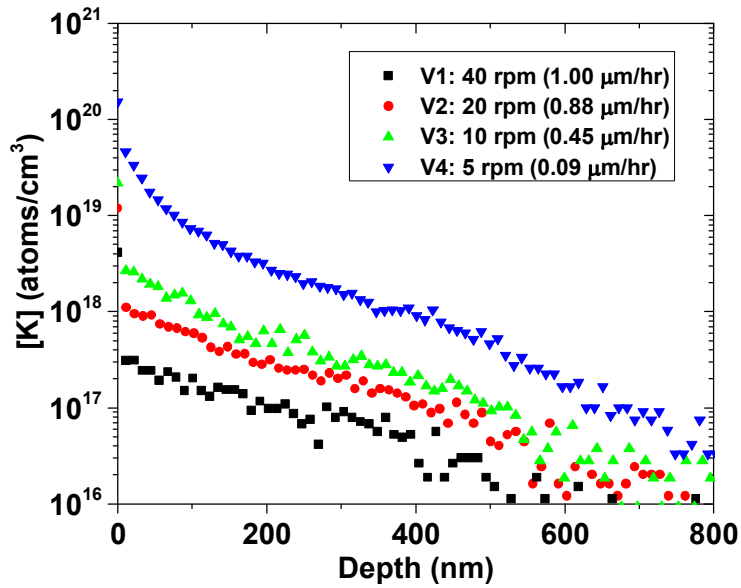
Series	Sample	Treatment	Pad	Slurry	pH	Rotation Rate (rpm)	Removal Rate ($\mu\text{m/hr}$)
Velocity	V1	Polish	MHN	Cerria: Stab. Hastilite PO	8.3	40	1.00
	V2					20	0.88
	V3					10	0.45
	V4					5	0.09
Pad	P1	Polish	MHN	Cerria: Stab. Hastilite PO	8.3	20	0.69
	P2		Chem-Poly				0.67
	P3		Optivision				1.71
	P4		Polytex 1				0.65
	P5		Polytex 2				0.90
Slurry	S	Polish	MHN	Cerria: NanoArc	8.3	20	1.12
	H1	Polish	MHN	Cerria: Stab. Hastilite PO	6		0.54
H2	8.3					0.88	
H3	10.5				20	0.95	
H4	12					1.08	
H5*	8.3					1.86	
No Polishing-Soak	NP1	Soak	NA	Cerria: Stab. Hastilite PO (2 wk)	8.3	NA	0
	NP2			KOH (2 wk)	13.7		0
	NP3			KOH (18hr)	13.7		0

*pad treated for higher removal rate

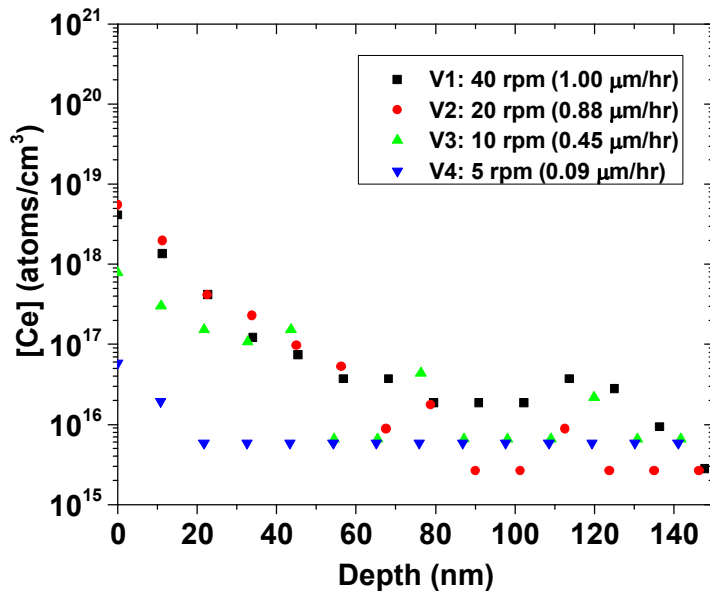
Table 2: Parameters used for developing chemical-mechanical-structural representation of the Bielby layer and polishing process.

Parameter	Symbol	Value	Si:X*	Source
Bielby layer thickness	l_{Bielby}	50 nm	-	This study
H surface concentration	$C_{\text{H-s}}$	2×10^{20} atoms/cm ⁻³	100:1	This study
Ce surface concentration	$C_{\text{Ce-s}}$	5×10^{19} atoms/cm ⁻³	400:1	This study
K surface concentration	$C_{\text{K-s}}$	1×10^{18} atoms/cm ⁻³	2000:1	This study
Bulk SiO ₂ Structure	Q ⁴ :Q ³ :Q ² :Q ¹	87:11:2:0	-	[25]
Surface SiO ₂ Structure	Q ⁴ :Q ³ :Q ² :Q ¹	86:12:2:0	-	This study
Removal rate	dh/dt	0.80 μm/hr	-	[14]
Particle Size	r	400 nm	-	[14]
Average Load/particle	P	10 ⁻⁴ N	-	[14]
Contact zone diameter	2a	110 nm	-	[14]
Elastic depth	d _e	3.8 nm	-	[14]
Removal depth	d	1 nm	-	[14]

*atomic ratio of Si (2×10^{22} atom/cm⁻³) to that of H, Ce or K

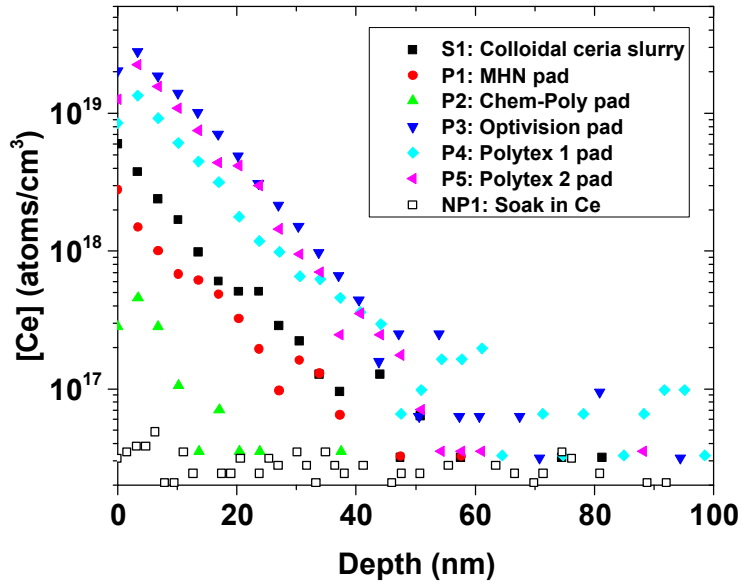


(a)

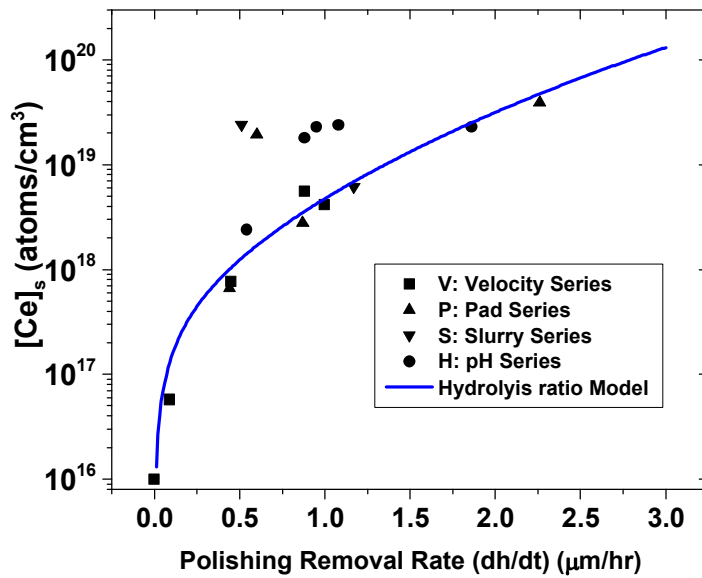


(b)

Figure 1: (a) SIMS generated depth profile of K on fused silica surfaces prepared at different material removal rates, measured 2 weeks after polishing; (b) SIMS generated depth profile of Ce on the same fused silica surfaces prepared at different material removal rates.

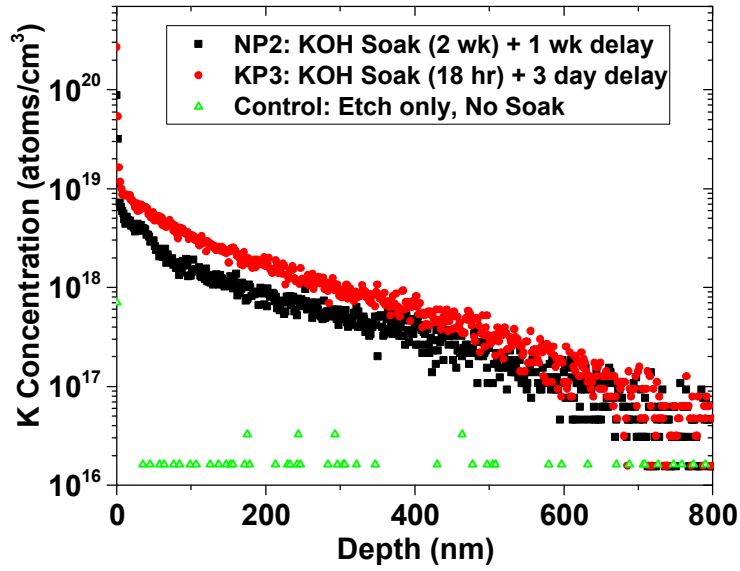


(a)

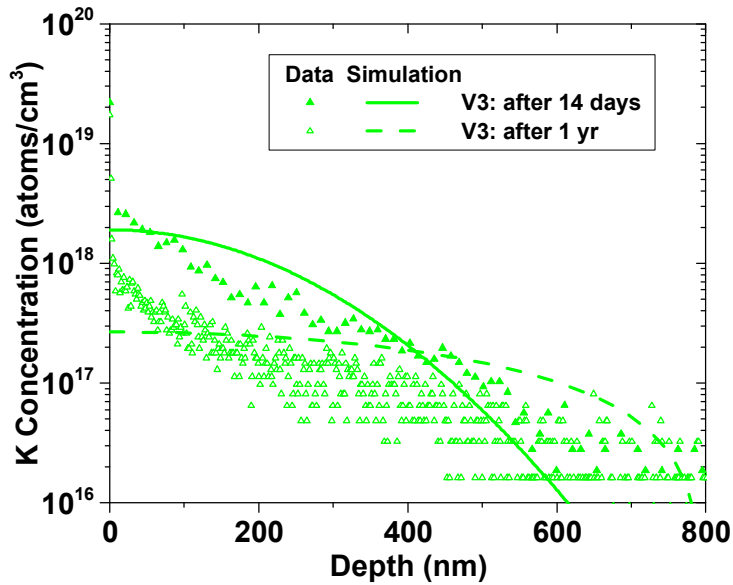


(b)

Figure 2: (a) SIMS generated depth profile of Ce on fused silica surfaces prepared under various polishing conditions; (b) Surface Ce concentration of the samples shown in Figs. 1a and 2b as function of polishing material removal rate (points are measured data and the line is the calculated value using the hydrolysis ratio model given by Eq. (10) using $r_0=80$ and $E=10$ kcal/mol (see text)).



(a)



(b)

Figure 3: (a) SIMS generated depth profile of K on etched fused silica surfaces that were soaked in aqueous KOH (b) SIMS generated depth profile of K for polished sample V3, two weeks after polishing and 1 yr after polishing. The lines are the calculated diffusion profiles using a simple one step diffusion model.

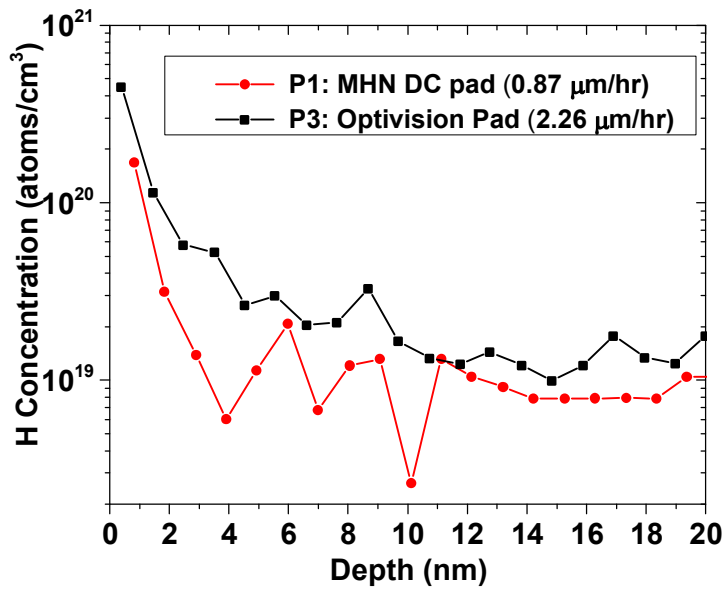


Figure 4. Depth profile of H surface, as measured by H SIMS, on selected polished fused silica surfaces.

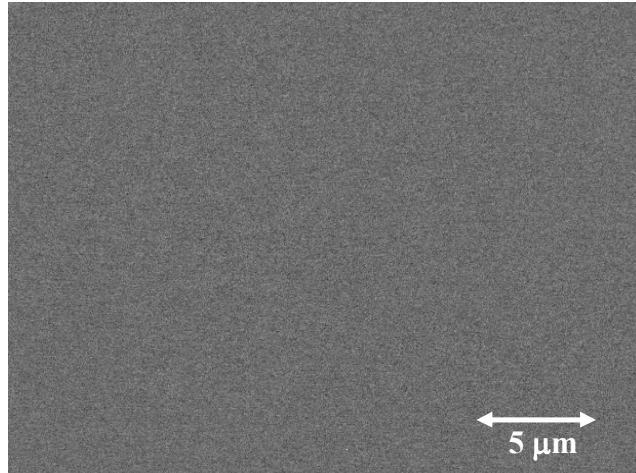


Figure 5: FE-SEM image of polished fused silica surface. The featureless image should to be compared with that taken by Liao [10].

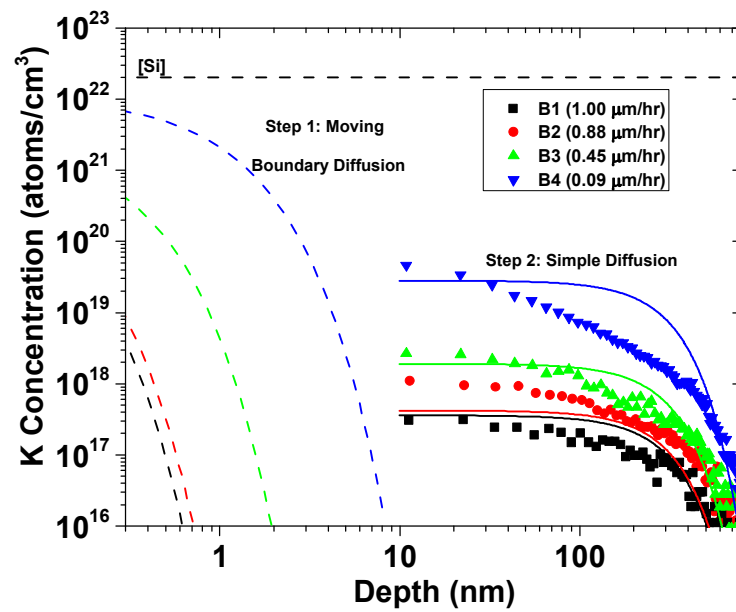


Figure 6: Comparison of the proposed two-step diffusion model with the measured depth profile of K. All measurements were performed two weeks after polishing.

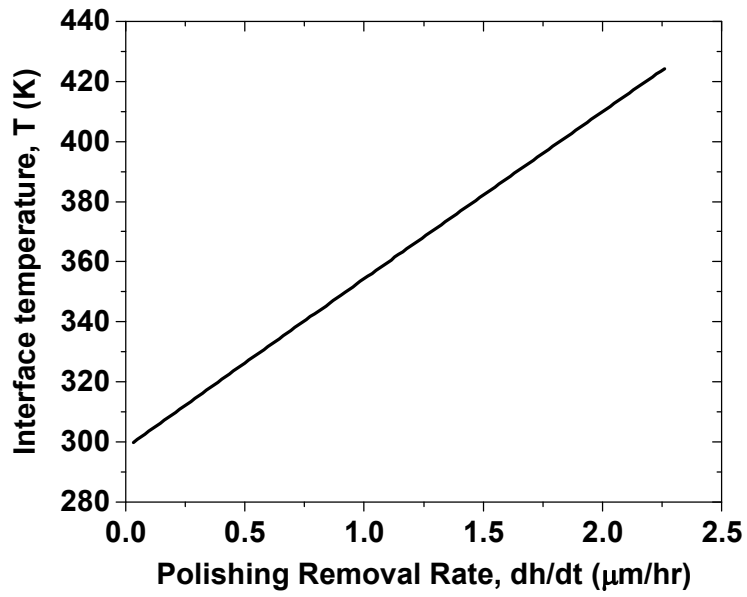


Figure 7: Calculated polishing particle – workpiece interface temperature as function of material removal rate (driven by particle velocity) using the Eqs. (2) and (9).

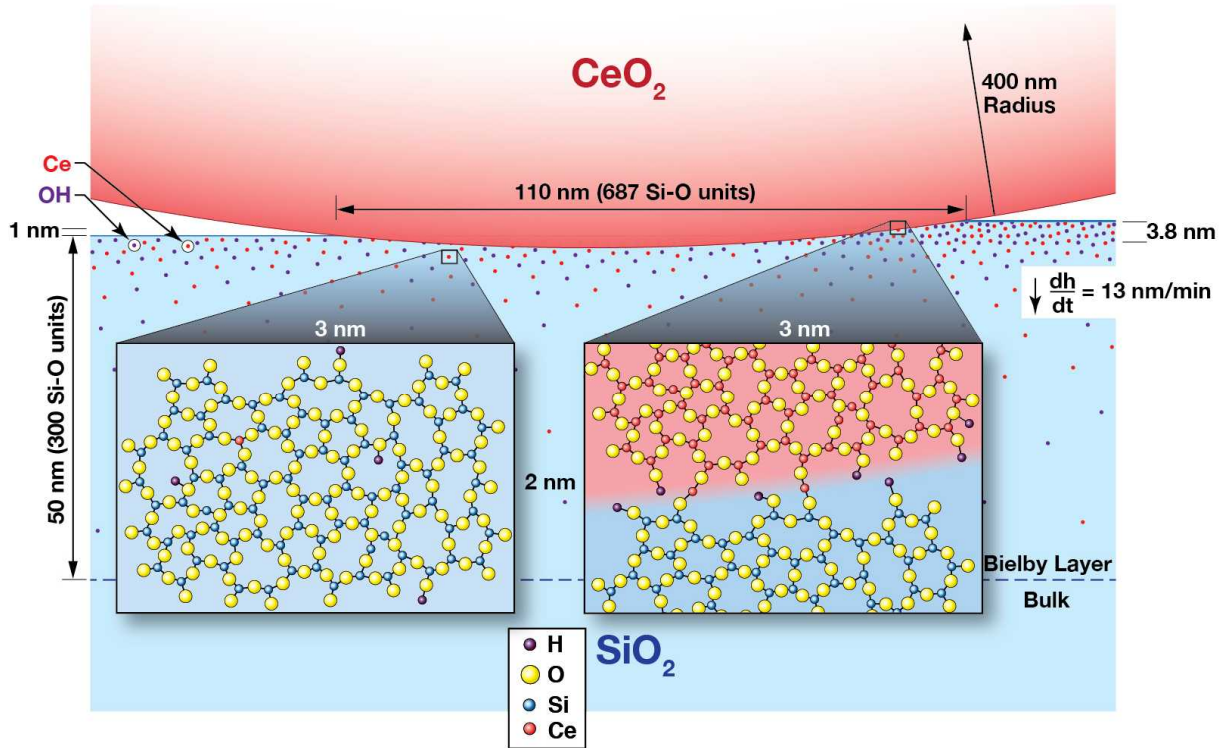


Figure 8: Schematic representation of proposed chemical and structural model of the polishing process and the Bielby layer.